Supporting Information

Hollow Spherical Nano-traps Using Pillararene-based Polymer for Efficient Uranium Extraction from Seawater

Qiang He,[a,c]† Jiehai Peng,[a]† Yumei Wang,[b] Guodong Sheng,[a] Na Chang,[d] Kui Du*[a], Yue Sun[b] and Haitao Wang*[d]

[a] *School of Chemistry and Chemical Engineering, Shaoxing University, Shaoxing 312000, PR China. E-mail: dkui@usx.edu.cn*

[b] *State Key Laboratory of Separation Membrane and Membrane Process, School of Chemistry, Tiangong University, Tianjin 300387, PR China.*

[c] *Key Laboratory of Pesticide and Chemical Biology (CCNU), College of Chemistry, Central China Normal University, Wuhan 430079 P. R. China*

[d] *State Key Laboratory of Separation Membrane and Membrane Process, School of Environmental Science and Engineering, Tiangong University, Tianjin, 300387, PR China. E-mail:* wanghaitao@tiangong.edu.cn

† *These authors equally contributed to this work.*

Supporting information for this article is given via a link at the end of the document.

Table of Contents

1. Materials and General Methods

Materials and Instruments

All chemicals from chemical suppliers were used without further purification. To synthesis pillar[5]arene with ten carboxyl groups (P5), the hydroquinone dimethyl (98 %), $(HCHO)_n$ (molecular weight: 30.02, 96 %), boron (III) fluoride etherate (98 %), boron tribromide (99.9 %) and ethyl bromoacetate (98 %) were purchased from Shanghai Macklin Biochemical Co., Ltd. All the solutions are purchased from Sinopharm Chemical Reagent Co., Ltd.

The morphology and elemental composition were studied using SEM (Hitachi SU-8010) X-ray photoelectron spectroscopy measurements were carried out on a Thermo Scientific Escalab Xi+, which had monochromatic Al Kα as the X-ray source. energy dispersive X-ray spectroscopy (EDS) mapping analyses were obtained using a JEM−ARM200F scanning transmission electron microscope operating at 200 kV and equipped with a spherical aberration corrector. Inductively coupled plasma mass spectrometry (ICP−MS) analyses were performed on a Shimadzu 2030 spectrometer system. FT-IR spectroscopy was conducted using a Thermo Nicolet Nexus 470. Thermogravimetric analysis was performed using a Netzsch TG209F3 from 40 to 700 °C under a nitrogen atmosphere. BET surface areas were determined from N_2 adsorption/desorption isotherms obtained at 77 K using a Micromeritics TriStar II. Solid-state nuclear magnetic resonance (NMR) spectra were recorded on a BRUKER 400WB AVANCE III spectrometer (B0 = 9.4T, lamor frequency 400.13 MHz for ^{1}H, 100.61 MHz for ^{13}C) at room temperature. UV–VIS spectra were taken on a PerkinElmer Lambda 35 UV–VIS spectrophotometer.

Uranium sorption in uranyl ion−spiked seawater

To determine the uranium adsorption kinetics in seawater, P5-AO was dispersed in 200 mL of uranyl−spiked seawater (10 ppm based on uranium, uranyl nitrate hexahydrate was used to prepare the solution, the pH of the uranyl−spiked seawater solution was adjusted by using sodium hydroxide to 8.1) at a good dispersion and then stirred with time. At increasing time intervals, 2 mL aliquots were removed from the mixture, filtered through a 0.45 μm membrane filter, and the filtrates were analyzed by UV–VIS spectra using the Arsenazo III Spectrophotometric method at 650 nm.

To obtain the adsorption capacities for P5-AO, the adsorbent was dispersed in 200 mL of uranyl−spiked seawater of varying uranium concentration (from 0 to 20 ppm based on uranium, the pH of the uranyl−spiked seawater solutions was adjusted by using sodium hydroxide to 8.1). The solutions were sonicated to achieve good dispersion and then shaken with time. Subsequently, the solutions were filtered through a 0.45 μm membrane filter, and the filtrates were analyzed by UV–VIS spectra using the Arsenazo III Spectrophotometric method at a wavelength of 650 nm (Figure S6). All the batch adsorption experiments were conducted three times and the error bars were used in the curves.

Adsorption kinetics and isotherms.

The pseudo−first−order kinetic model and pseudo−second−order kinetic model were applied to fit the adsorption data:

$$\ln\left(q_e - q_t\right) = lnq_e - lnK_1 t$$

$$\frac{t}{q_t} = \frac{1}{K_2 q_e 2} + \frac{t}{q_e}$$

where k_1 (min^{-1}) and k_2 ($g \cdot mg^{-1} \cdot min^{-1}$) are the rate constants of pseudo−first−order and pseudo−second−order kinetic models, q_e and q_t are the amounts of adsorbed uranyl ions ($mg \cdot g^{-1}$) at equilibrium and a given time (t, min), respectively.

The Langmuir and Freundlich equation shown below was also used to evaluate the uranium adsorption capacity of the adsorbents. The uranium uptake capacity of the P5-AO was analysed by the Langmuir model and Freundlich model:

$$\frac{C_e}{q_e} = \frac{C_e}{q_m} + \frac{1}{K_3 q_m}$$

$$q_e = K_4 C_e^{\frac{1}{n}}$$

where C_e is the equilibrium concentration, q_e is the adsorption capacity of uranium in the equilibrium state, q_m is the maximum adsorption capacity, and K_3 and K_4 are the equilibrium constants related to the binding strength.

Determination of optimal adsorption pH for uranium uptake.

The optimal adsorption pH was investigated by using 8 ppm uranyl nitrate simulate seawater and ultrapure water solution with different pH values. The making method of stimulated

seawater comprises the following steps: adding 184.62 × 10^{-3} M sodium chloride and 2.30 × 10^{-3} M sodium bicarbonate in ultrapure water to make simulate seawater. The pH of the uranium solutions was adjusted by dilute sodium hydroxide and dilute hydrochloric acid, and the pH ranges from 3.0 to 9.0. Then 5 mg adsorbents were dispersed into 500 mL 8 ppm uranium spiked solutions. After shaking at room temperature for 24 hours achieved the adsorption/desorption equilibrium, the concentration of centrifuged solutions was determined by UV–VIS spectra. The adsorption capacity of qt (mg g^{-1}) is obtained by the following formula:

$$q_t = \frac{(C_0 - C_e) \times V}{m}$$

where C_0 (mg L^{-1}) represents the initial concentration of uranium, C_e (mg L^{-1}) represents the equilibrium concentration of uranium after centrifuged, V (L) represents the volume of the solution and m (g) represents the mass of adsorbent.

Determination of reusability and binding selectivity.

Five consecutive adsorption/desorption cycles were performed to study the reusability and selectivity of the P5-AO adsorbents in simulated seawater. Six metal ions were added to natural seawater to prepare the solution. The concentrations of U, V, Ni, Cu, Fe, Pb and Cd were 100 times those in natural seawater. The pH value was adjusted to 8.1 ± 0.3 using NaOH. Subsequently, 10 mg of the hollow spherical polymers was placed in 200 mL of the above solution for 24 h at 25°C. The adsorption capabilities for different ions were determined by ICP-MS. The ion-loaded adsorbents were then regenerated by immersion in an eluent (20 ml of 0.5 M HCl solution) with stirring at 25°C for 1 h. After elution, the adsorbents were regenerated in an alkaline solution (20 ml of 5 mM NaOH) for 15 min and then used for the next cycle. The elution efficiency was calculated according to the concentration of ions in the eluent determined by ICP-MS.

The bacterial resistance experiment of P5-AO.

Experimental Procedure: Escherichia coli was selected as the representative bacterium for antibacterial testing. Firstly, a certain concentration of live Escherichia coli was cultured and then diluted to an ultraviolet optical density (**OD**) of approximately 0.1. Using a pipette, 100 μL of the diluted bacterial suspension was evenly spread on a nutrient agar plate. The material was placed in the center of the petri dish for bacterial culture and incubated for 12 hours. Subsequently, antibacterial activity was determined by measuring the radius of the inhibition zone according to methods reported previously.[1,2] For ease of observation and comparison of the materials' antibacterial properties, 0.01g, 0.03g, 0.05g, 0.08g, and 0.1g of P5-AO were separately weighed and adsorbed onto wooden discs with a radius of 0.6 cm for the experiment.

2. Synthesis of Carboxyl Pillar[5]arene (P5).

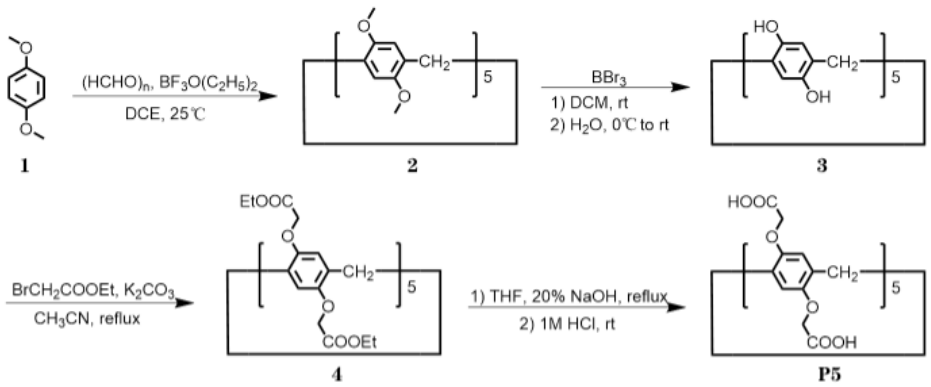

Scheme S1. Synthesis of the **P5**

Compound 2

To synthesis compound **2**, an oven-dried flask equipped with a magnetic stir bar, $(HCHO)_n$ (72.4 mmol, 2.2g) and **1** (72.4 mmol, 10g). The flask was evacuated and backfilled with argon (repeat three times). Then $BF_3O{\cdot}(C_2H_5)_2$ (72.4 mmol, 9 mL) and dichloroethane (DCE,100 mL) were added into the flask. The resulting mixture was stirred at 25˚C for 1 hour and the colour became black. After finished the mixture was filtered and washed with DCE three times, and the liquid phase was concentrated in vacuo and residue was purified with column chromatography on silica gen using petroleum ether/CH_2Cl_2 as eluent to give the compound **2** (9.41g, yield at 86%).

Compound 3

To synthesis **3**, compound **2** (4 mmol, 3g) was dissolved into dichloromethane (DCM, 100mL) and add BBr_3 (41mmol, 4mL) then stir for 72 hours in room temperature. After this slowly input ice water and continue stir for 36 hours then wash and flitter the solid compound **3** (2.3g, yield at 92%).

Compound 4

To synthesis compound **4**, dissolve the **3** (3.7 mmol, 2.3g) in acetonitrile (100 mL) with K_2CO_3 (248 mmol, 35g) and heat to reflux. After the solvent boiled add $BrCH_2COOCH_2CH_3$ (124 mmol, 13.72g) dropwise and keep the mixture reflux for 48 hours. After the reaction finished

flitter and wash with acetonitrile, and the liquid was concentrated in vacuo and purified with column chromatography on silica gen using petroleum ether/CH_2Cl_2 as eluent to give the compound **4** (4.3g, yield at 79%).

Synthesis of P5

To synthesis **P5**, dissolve compound **4** (2 mmol, 3 g) in THF (70 mL) and add 20% NaOH aq (30 mL) then heat to reflux for 15 hours. After this distilled THF and add H_2O (70 mL), then add HCl aq (1M) dropwise adjust pH to 7. Then flitter and wash the solid with water and get solid **P5** (2.2g, yield at 93%). ^{1}H NMR (600 MHz, DMSO-d_6) δ (ppm): 12.96 (s, 10H), 7.11 (s, 10H), 4.71–4.68 (d, J = 15.9 Hz, 10H), 4.43–4.40 (d, J = 15.8 Hz, 10H), 3.74 (s, 10H).

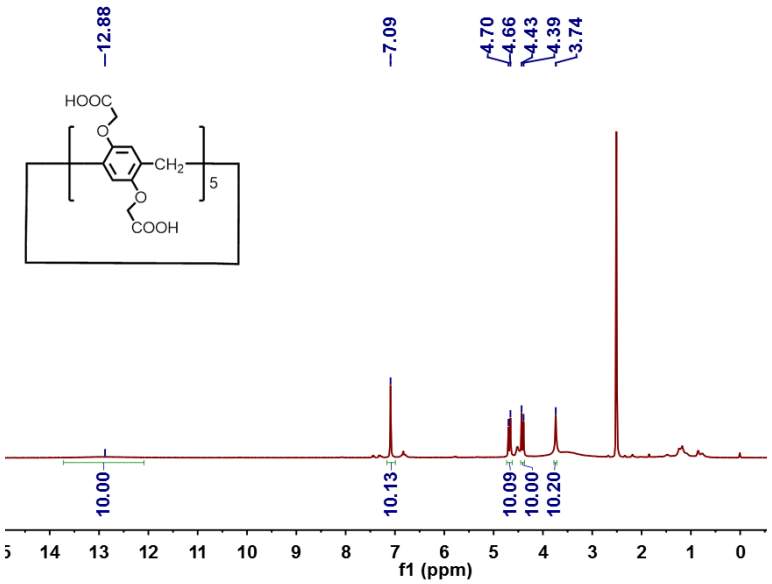

Figure S2. ^{1}H NMR spectroscopy of **P5** (600 MHz, DMSO-d_6)

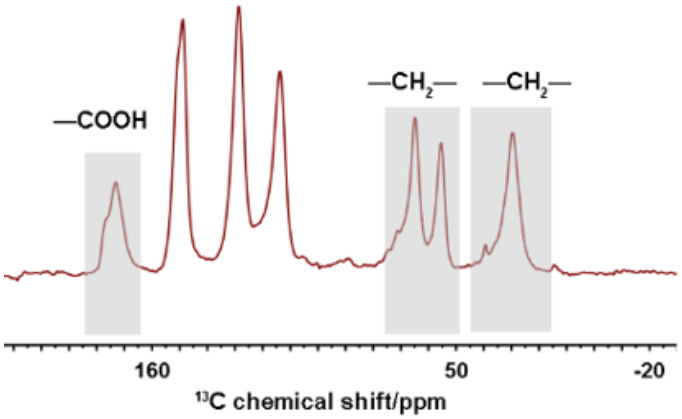

Figure S3. (a) ^{13}C CPMAS NMR spectra of **P5**. (b) SEM of **P5**

3. Synthesis and functionalization of porous polymers

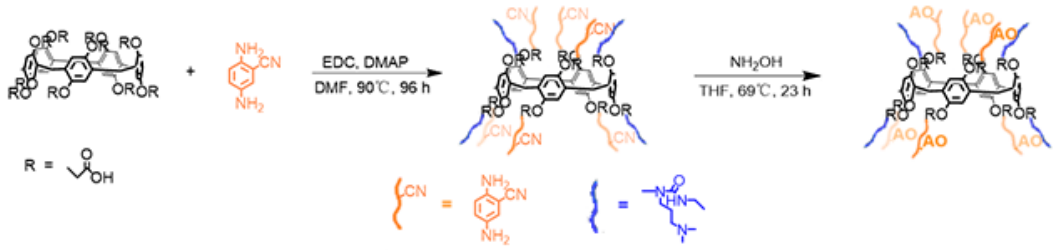

Figure S4. The synthesis process of **P5-AO**

The compound P5 (1.13 g, 1.00 mmol), p-phenylenediamine (**Db**) (0.320 g, 3.00 mmol), 1-(3-dimethylaminopropyl)-3-ethylcarbodiimide hydrochloride (**EDC**) (2 g, 10.0 mmol), 4-dimethylaminopyridine (**DMAP**) (0.06 g, 0.500 mmol), and DMF (100 mL) were added into a 250 mL round bottom flask. The reaction mixture was stirred at 95 °C for 96 hours under argon. After the reaction, the solvent was removed. The solid was washed with H_2O (100 mL), alcohol (100 mL), and actone (100 mL). Then, the solid was dried under high vacuum to yield the product, P5-Db, as a brown powder (1.26 g, 70% yield).

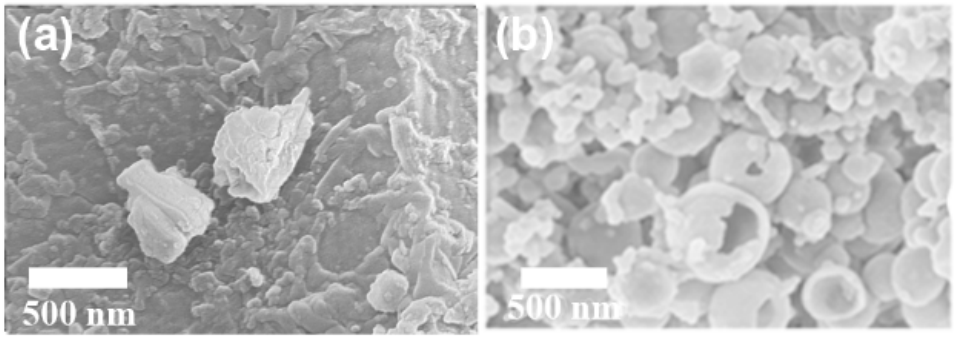

Figure S5. SEM of P5 (a) and P5-AO (b)

To synthesis polymer **P5-AO**, the **P5-Db** powder (1.8 g) was dissolved in tetrahydrofuran (120 mL) and heated to 69°C. Hydroxylamine solution (14 mL, 50 wt% in H_2O) was added drop by drop, and the reaction was then refluxed for 23 h under N_2. The yellow solution was poured into ethanol (500 mL) after being cooled to room temperature, and the precipitated polymer was then washed by ethanol several times. The brown product was dried at 100°C for 12h.

4. The liner regression fitting of uranium

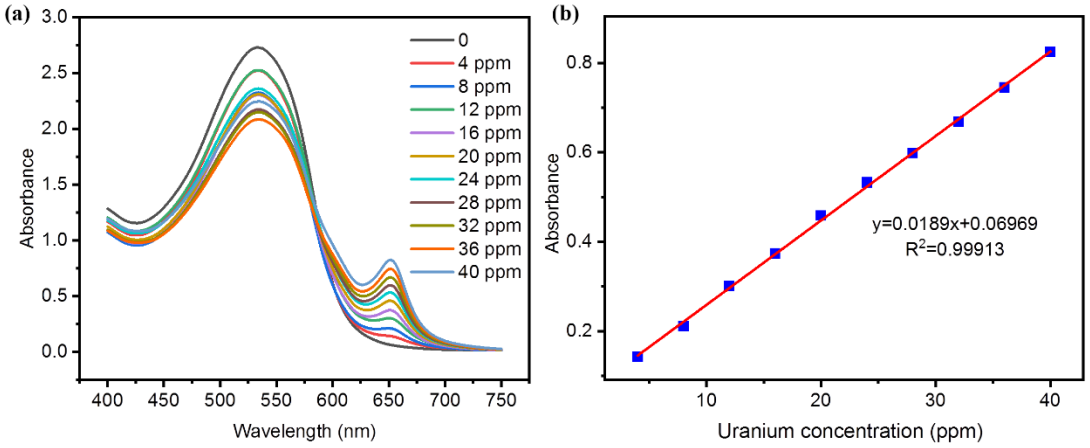

Figure S6. (a) Ultraviolet-visible absorption spectrum of uranyl in Arsenazo (III) standard solutions. (b) The liner regression fitting of concentration-absorbance in Arsenazo (III) standard solutions with different uranium concentration

5. N_2 sorption isotherms of polymers based P5

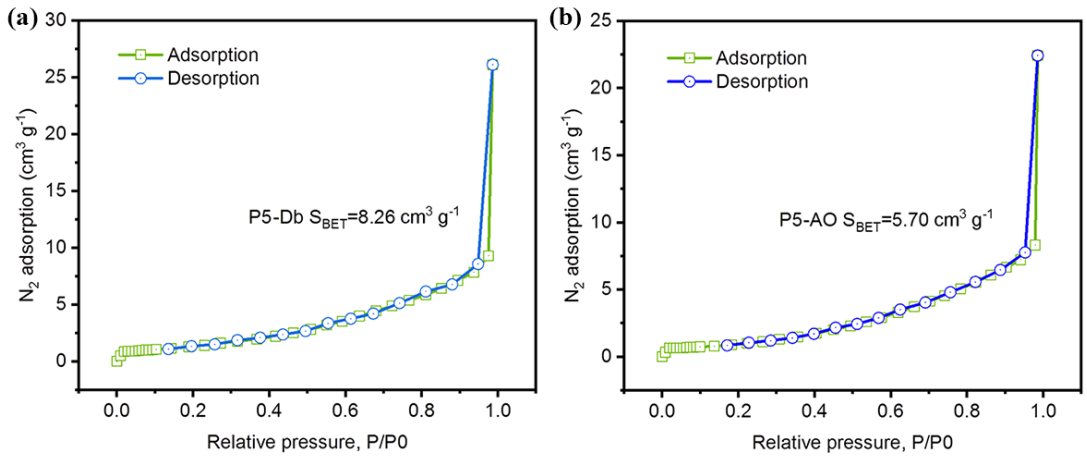

Figure S7. N_2 sorption isotherms collected at 77 K. The BET surface area of P5-Db and P5- AO were calculated to be 8.26 cm^3 g^{-1} (a) and 5.70 cm^3 g^{-1} (b), respectively

6. X-ray Photoelectron Spectroscopy of U@P5-AO adsorbents

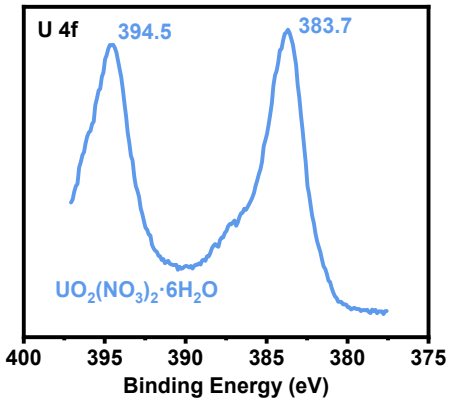

Figure S8. U4f XPS spectrum of $UO_2(NO_3)_2·6H_2O$

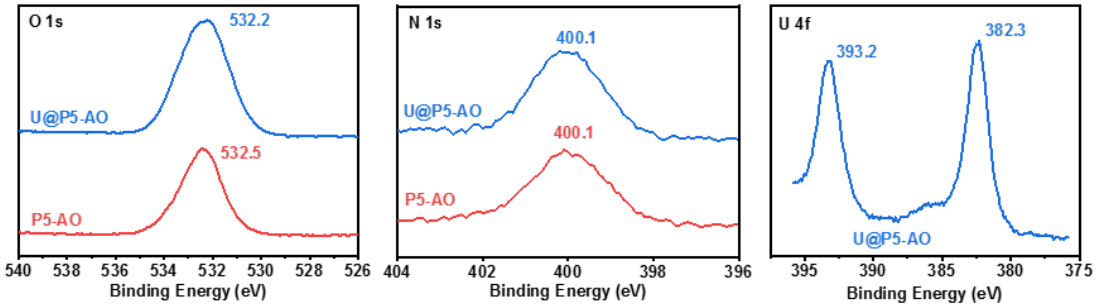

Figure S9. O1s, N1s, and U4f XPS spectra

7. DFT calculation of U@P5-AO coordination mechanism

All calculations in this work were performed using Gaussian 09 program package. Full geometry optimizations were performed to locate all the stationary points, using the PBE0[1] with the SDD[2-3] basis for U, and 6-31G* for C, H, O, and N. Dispersion corrections were computed with Grimme's D3(BJ) method in optimization[4]. Harmonic vibrational frequency was performed at the same level to guarantee that there is no imaginary frequency in the molecules, i.e. they locate on the minima of potential energy surface[5]. Convergence parameters of the default threshold were retained (maximum force within 4.5×10^{-4} Hartrees/Bohr and root mean square (RMS) force within 3.0×10^{-4} Hartrees/Radian) to obtain the optimized structure. The optimal structure was identified given that all calculations for structural optimization were successfully converged within the convergence threshold of no imaginary frequency, during the process of vibration analysis. The most stable structures of the complexes are shown below.

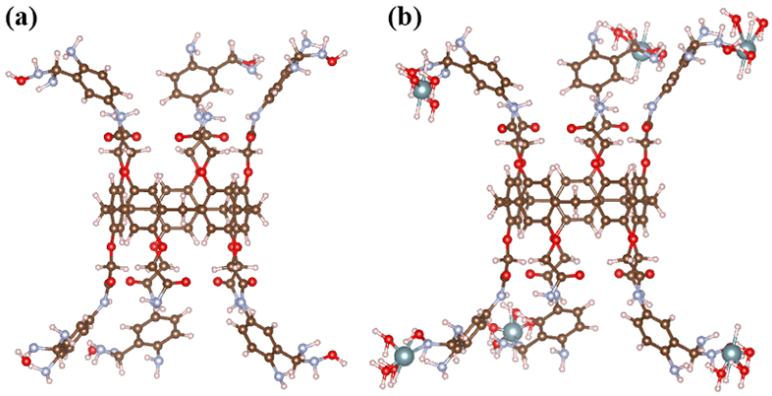

Figure S10. The most stable structures of (a) **P5-AO** and (b) UO_2(**P5-AO**)

1. R. Krishnan, J. S. Binkley, R. Seeger, J. A. Pople, *J. Chem. Phys.* 1980, **72**, 650-654.
2. F. Weigend, R. Ahlrichs, *Phys. Chem. Phys.* 2005, **7**, 3297-305.
3. S. Xu, T. He, J. Li, Z. Huang, & C. Hu, *Appl. Catal. B: Environ.* 2021, **292**, 120145.
4. S. Grimme,; J. Antony, S. Ehrlich, H. Krieg, *J. Chem. Phys.* 2010, **132**, 154104.
5. C. Gonzalez, H. B. Schlegel, *J. Chem. Phys.* 1989, **90**, 2154-2161.

8. Photos of P5-AO adsorbent materials

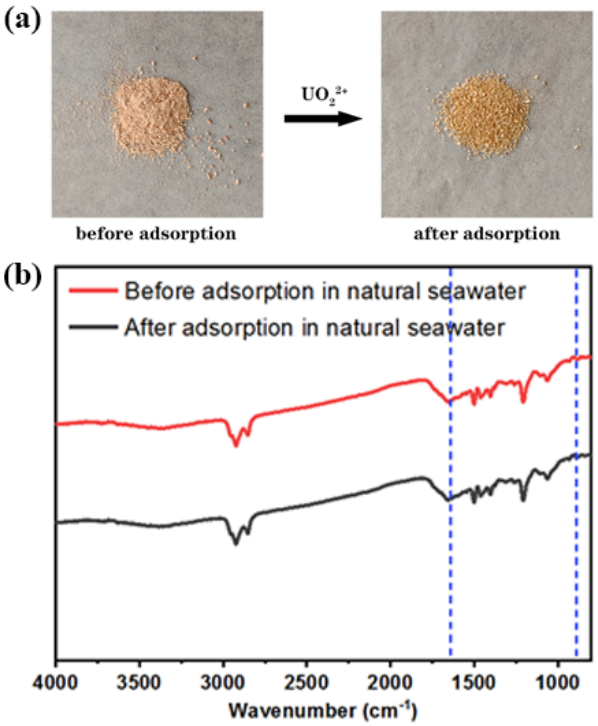

Figure S11. (a) Photos of **P5-AO** adsorbent materials before and after uranium inclusion. (b) FT-IR spectra of **P5-AO** before and after adsorption in natural seawater

9. The bacterial resistance experiment of P5-AO

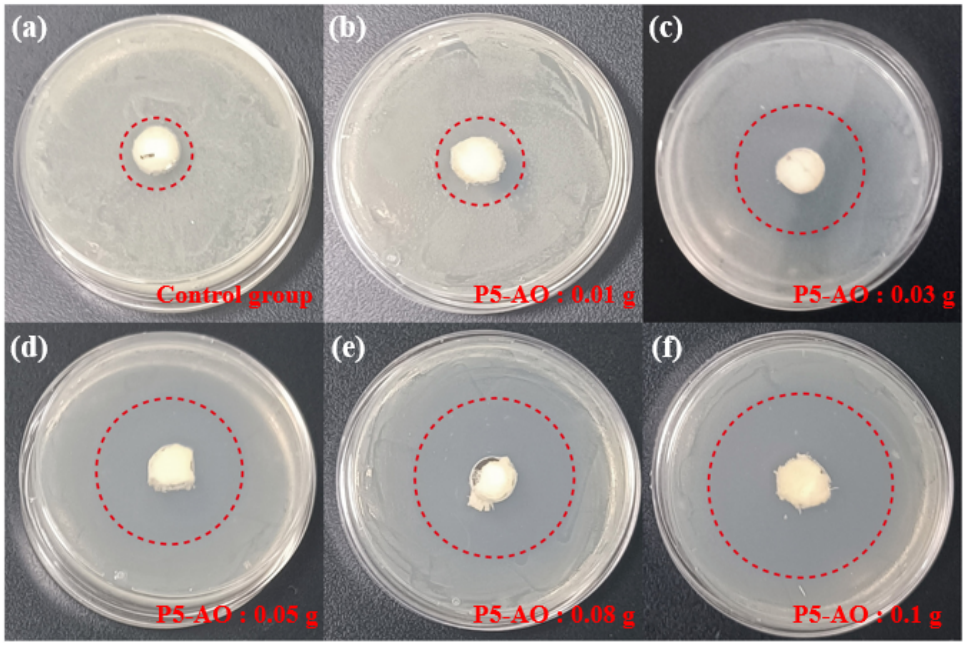

Figure S12. Escherichia coli antibacterial activity experiment of **P5-AO** (a) Control group without addition of **P5-AO**. (b) 0.01 g addition of **P5-AO**. (c) 0.03 g addition of **P5-AO**. (d) 0.05 g addition of **P5-AO**. (e) 0.08 g addition of **P5-AO**. (f) 0.1 g addition of **P5-AO**.

10. EXAFS analysis of U@P5-AO coordination environment

Sample Preparation.

Approximately 20-25 mg of the sample was encapsulated within a nylon washer with an inner diameter of 4.953 mm (area of 0.193 cm^2), and sealed on one side with transparent "Scotch" tape. The sample was thoroughly compressed by hand to form a solid, uniform pellet, then sealed on the open side with a second piece of tape. The entire assembly was placed into a Mylar bag. Small pieces of Kapton tape were employed to seal the three open edges of the Mylar bag. This methodology received prior approval from the APS Radiation Safety Review Board for the analysis of radioactive samples, fulfilling the requirements for dual containment.

Data Collection.

X-ray absorption data were collected at the BL14W1 beamline at the Shanghai Synchrotron Radiation Facility. Spectra were acquired at the uranium L3-edge (17166 eV) in transmission mode. The X-ray white beam was monochromatized using a Si (111) monochromator and detuned by 50% to minimize the contribution of higher-order harmonics to below the noise level. The K-edge of a yttrium foil (17038 eV) served as the reference for energy calibration and was measured simultaneously for all samples. The intensities of the incident beam (I_0), transmitted beam (I_t), and reference (I_r) were measured by 20 cm ionization chambers filled with gas mixtures of 80% N_2 and 20% Ar, 95% Ar and 5% N_2, and 100% N_2, respectively. All spectra were collected at room temperature. Samples were aligned at the center of the beam and adjusted to locate the most homogeneous section of the sample for data collection. The beam dimensions were reduced to 400 × 3100 μm for all data collection efforts. Data collection spanned six regions: -250 to -30 eV (step size 10 eV, dwell time 0.25 seconds), -30 to -5 eV (step size 5 eV, dwell time 0.5 seconds), -5 to 30 eV (step size 1 eV), 3 Å-1 to 6 Å-1 (step size 0.05 Å-1, dwell time 2 seconds), 6 Å-1 to 9 Å-1 (step size 0.05 Å-1, dwell time 4 seconds), and 9 Å-1 to 15 Å-1 (step size 0.05 Å-1, dwell time 8 seconds), with three scans collected for each sample.

The data underwent processing and analysis via the Athena and Artemis software components within the IFEFFIT suite, leveraging the computational framework of FEFF 6. Calibration of the reference foil was meticulously aligned with the initial zero-crossing observed in the second derivative of the μ(E) data, normalized to conform precisely to the documented E0

value for the yttrium L3-edge (17166 eV). Prior to normalization, spectral data were consolidated by averaging the μ(E) values. Subsequently, the background was meticulously subtracted from the dataset, and a background subtraction coefficient (Rbkg) was uniformly set to 1.0, ensuring consistency across the analysis.

Fitting.

Initial data fitting utilized k-weights of 1, 2, and 3 to assess structural parameters broadly. Subsequently, a more refined analysis was conducted in R-space, employing K2 and K3 weights for a nuanced interpretation. Key structural parameters determined included the multiplicity of scattering paths (Ndegen), modifications in half-path lengths (ΔRi), the comparative mean-square displacement among scattering elements (σ^2i), the passive electron attenuation factor (S_{o2}), and adjustments in the photoelectron energy (ΔE_o). For consistency across all models, S_{o2} was maintained at a fixed value of 1. To adhere to the Nyquist criterion, the count of independent data points was carefully capped at two-thirds of the total variables for each analysis iteration. The approach to fitting was methodical, starting from fundamental parameters and progressing to more complex ones, including the calibration of atomic multiplicities through a scalable factor affecting S_{o2}. This progressive inclusion of extended scattering paths utilized refined estimates from established paths as preliminary inputs, permitting adjustments to ensure accuracy without the introduction of systemic biases. The comprehensive fitting models incorporated three principal scattering trajectories of axial oxygen, indicative of a dynamic count of carbon scatterers positioned at 2.90 Å, characteristic of carbonate structures.

11. Supplementary Tables

Table S1 EXAFS analysis of UO_2(P5-AO).

Element	Path	N	S_0^2	σ^2(Å^2)	R(Å)	R-factor
U	U-O	2	1	0.0027(0.0031)	1.76(0.03)	0.004
	U-O	3.2(0.74)	1	0.0044(0.0091)	1.99(0.08)	
	U-O	1.5(0.28)	1	0.0120(0.0038)	2.46(0.03)	
	U-C	3.5(0.7)	1	0.0078(0.0048)	2.90(0.05)	

Table S2. Selected bond lengths (A) of the UO_2(P5-AO) complexes calculated at the M06/SSC/6-311++G(d,p) level in comparison with the EXAFS results of UO_2(P5-AO).

	EXAFS UO_2(P5-AO)	M06/SSC/6-311++G(d,p) UO_2(P5-AO)
U-O(UO_2^{2+})	1.76	1.76
U-O(H_2O)	1.99	1.99
U-O(oximate group)	2.46	2.44
U-N(oximate group)	2.46	2.45

Table S3. Uranium sorption performance of representative adsorbents in the literature.

Adsorbents	Water (mg g^{-1})	Artificial seawater (mg g^{-1})	Seawater (mg g^{-1})	The average daily adsorption amount in seawater (mg g-1)
MUU*im*[a]	--	475	7.35	0.46
POP-*o*NH_2-AO[b]	--	530	4.36	0.08
Mesoporous Carbon Materials[c]	97	67	--	--
Sx-LDH[d]	330	--	--	--
COF hydrogel (CPP)[e]	--	--	4.15	0.42
HOF-1[f]	--	--	17.9	0.60
FJSM-SnS[g]	338	--	--	--
BP@CNF-MOF[h]	--	288.8	6.77	0.16
PPH-OP[i]	--	139.47	7.12	0.34
AO-PIM-1[j]	--	390.0	9.03	0.32
PAO hydrogel[l]	--	1279.0	4.87	0.17
P5-AO (this work)	--	139.5	8.1	0.45

[a] L. J. Feng, H. Wang, T. T. Feng, B. J. Yan, Q. H. Yu, J. C. Zhang, Z. H. Guo, Y. H. Yuan, C. X. Ma, T. Liu, N. Wang, *Angew. Chem. Int. Edit*. 2021, **61**, 16110–16114.

[b] Q. Sun, B. Aguila, J. Perman, A. S. Ivanov, V. Bryantsev, L. Earl, C. W. Abney, L. Wojtas, & S. Q Ma, *Nat. Commun.* 2018, **9**, 1644.

[c] M. Carboni, C. W. Abney, K. M. L. Taylor-Pashow, J. L. Vivero-Escoto, & W. Lin, *Ind. Eng. Chem.*

Res. 2013, **52**, 15187-15197.

[d] S. Ma, L. Huang, L. Ma, Y. Shim, S. M. Islam, P. Wang, L.-D. Zhao, S. Wang, G. Sun, X. Yang, & M. G. Kanztzidis, *J. Am. Chem. Soc.* 2015, **13**, 3670-3677.

[e] W. R. Cui, C. R. Zhang, R. P. Liang, J. D. Qiu, *J. Mater. Che*m. *A*. 2021, **9**, 25611.

[f] A. Kaushik, K. Marvaniya, Y. Kulkarni, D. Bhatt, J. Bhatt, M. Mane, E. Suresh, S. Tothadi, K. Patel, S. Kushwaha, *Chem*. 2022, **8**, 1–17.

[g] M.-L. Feng, D. Sarma, X.-H. Qi, K.-Z. Du, X.-Y. Huang, & M. G. Kanatzidis, *J. Am. Chem. Soc.* 2016, **138,** 12578-12585.

[h] M. W. Chen, T. Liu, X. B. Zhang, R. Q. Zhang, S. Tang, Y. H. Yuan, Z. J. Xie, Y. J. Liu, H. Wang, K. V. Fedorovich, N. Wang, *Adv. Funct. Mater.* 2021, **31**, 2100106.

[I] Y. H. Yuan, Q. H. Yu, M. Cao, L. J. Feng, S. W. Feng, T. T. Liu, T. T. Feng, B. J. Yan, Z. H. Guo, N. Wang, *Nat. Sustain.* 2021, **4**, 708–714.

[j] L. S. Yang, H. Y. Xiao , Y. C. Qian, X. L. Zhao, X. Y. Kong, P. Liu, W. W. Xin, L. Fu, L. Jiang, L. P. Wen, *Nat. Sustain.* 2022, **5**, 71–80.

[l] C. X. Ma, J. X. Gao, D. Wang, Y. H. Yuan, J. Wen, B. J. Yan, S. L. Zhao, X. M. Zhao, Y. Sun, X. L. Wang, N. Wang, *Adv. Sci.* 2019, **6**, 1900085.